UNITED STATES DEPARTMENT OF INTERIOR
GEOLOGICAL SURVEY

URANIUM IN WHEELER BASIN
GRAND COUNTY, COLORADO

By

Edward J. Young

Open-File Report 82-730
1982

Table of Contents

Figures

Tables

ABSTRACT

Two kinds of radioactive anomalies are found in Wheeler Basin, both of which consist of biotite concentrations in Precambrian rocks, but the ones in migmatized biotite gneiss contain uraninite and the ones in Silver Plume Granite probably do not. At least 18 new uranium occurrences were found, most of which are less than a square meter. These discoveries enlarge the uraniferous area reported by Young and Hauff in 1975. Uranium in these biotite concentrations occurs in several modes: as uraninite grains; in accessory minerals, such as zircon; in fractures in plagioclase; and along grain boundaries and in cleavage openings in mica. Uranium mineralogy in the fractures, grain boundaries, and micas is not known. Yellow, secondary uranium minerals are seen locally on outcrop. Relative to crustal abundance, the radioactive biotite concentrations in migmatized biotite gneiss show depletion in Ca, Sr, Na, and, locally, Cu, but pronounced enrichment in U and Mo, and moderate enrichment in Pb, Ag, Th, and REE. The radioactive biotite concentrations in the Silver Plume Granite show pronounced enrichment in Th, and moderate enrichment in U, Sn, Zr, and Ag. Enrichment in light REE predominates over heavy REE. As U is more abundant in biotite concentrations in migmatized biotite gneiss than in biotite concentrations in Silver Plume Granite, I have concluded that U in the migmatized biotite gneiss was present before intrusion of the Silver Plume Granite, and that metamorphic effects of the Silver Plume intrusion remobilized U to form pockets of enrichment (biotite concentrations).

INTRODUCTION

Wheeler Basin is just west of the Continental Divide, about 20 airline miles (32km) west of Boulder, Colorado, and is a U-shaped, glacially scoured valley, tributary to the larger glacially scoured valley of Arapahoe Creek, which flows into Monarch Lake and thence into Lake Granby.

The disseminated uraninite that occurs in and around the Bennett adit shown in Figure 1 has been described by Young and Hauff (1975), and Ludwig and Young (1975) have dated the formation of the uraninite and associated monazite at 1446 ± 20 m.y., which correlates well with intrusion of the Silver Plume Granite. A broader, regional study of the area of Figure 1 and surrounding area has recently been published by Pearson and Johnson (1980). Some of their samples provide additional data for this report.

In 1977 the author and Richard I. Grauch spent three days in Wheeler Basin looking for a reported occurrence or occurrences of apatite-rich concentrations (80 percent apatite) in the Silver Plume Granite. Biotite concentrations enriched in monazite (thorium-bearing) were found instead, but some of the biotite concentrations contained as much as 6 percent apatite.

In 1980 three days were again spent in Wheeler Basin, and that field trip formed the basis for this report.

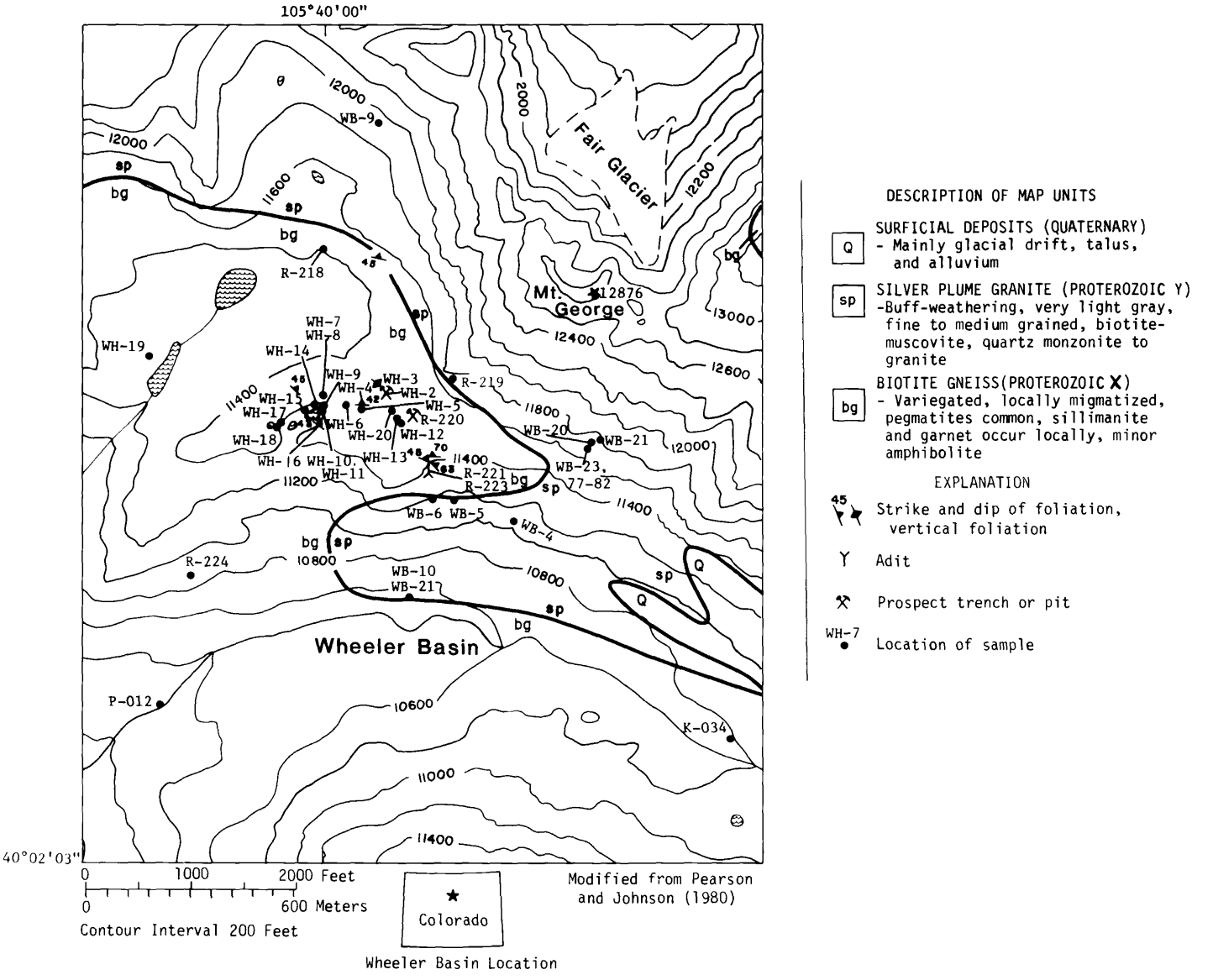

Figure 1.--Geology of the Wheeler Basin area.

GENERAL GEOLOGY

The uraniferous occurrences in Wheeler Basin are found in Precambrian metamorphic rocks consisting of migmatized biotite gneiss, mixed gneiss and pegmatite, and small but discrete pegmatites. These metamorphic rocks are part of the pre-1,700-m.y. metamorphic complex in Colorado (Tweto, 1977). Regional foliation in the metamorphic rocks generally strikes northwest to west northwest and dips northeast at moderate to steep angles (Fig. 1). A large pluton of Silver Plume Granite lies to the northeast of the occurrences, which all lie within, or close to, a triangular reentrant of the migmatized biotite gneiss into Silver Plume Granite. Close to, and parallel to, the northwest-trending contact of Silver Plume Granite and migmatized biotite gneiss are several steeply-dipping joint planes or fractures in the migmatized biotite gneiss that are stained with limonite. They are roughly parallel to the Arapahoe Pass Fault, about 3 miles (5km) to the south (Pearson and Johnson, 1980).

ECONOMIC GEOLOGY

Although the occurrences described herein are not economic because of insufficient size and relative inaccessability, this type of uranium concentration merits further study for at least two reasons: (1) not much is known about this type of occurrence, and (2) this concentration process is petrogenetically important. The radioactive anomalies in Wheeler Basin may be divided into two types: (1) anomalies in which uranium predominates in the migmatized biotite gneiss and (2) anomalies in which thorium predominates in the Silver Plume Granite.

Uranium anomalies in the migmatized biotite gneiss

At least 18 new uranium occurrences in Wheeler Basin were found in 1980, thus extending the uraniferous area described by Young and Hauff (1975). The new occurrences, shown in Figure 1 and listed in Table 1, are all small, usually less than a square meter. The few larger ones are inhomogeneous, the more radioactive areas within them being much smaller than a square meter. Figure 2 shows photographs of 10 occurrences. Of the 18 occurrences, 15 are uraniferous biotite concentrations in migmatite or pegmatite and three are radioactive fractures, either in pegmatite or in lenses of Silver Plume Granite.

Radiometric readings* from all the occurrences and uranium and thorium analyses of samples from 12 of the occurrences are given in Table 1. Chemical analyses of five radioactive biotite concentrations and of one radioactive Silver Plume Granite sample may be found in Table 2, and Table 3 lists spectrographic analyses of 11 of the occurrences.

Almost invariably the occurrences show high U/Th ratios. Only one, WH-10, is near unity. The range in uranium values is from 76 to 9,680 ppm.

*All radiometric data were taken with a Mount Sopris scintillometer, Model SC-132.

Table 1.--U and Th Analyses from Wheeler Basin. [Localities shown on Fig. 1. Radioactivity recorded by scintillometer in counts/sec (c/s). Uranium and thorium analyses by delayed neutron method except as noted. Analysts: H. T. Millard, Jr., R. Bies, B. Keaten, M. Coughlin, S. Lasater, D. M. McKown, J. Storey, S. Danahey, B. Vaughn, and J. S. Leventhal. -, leader indicates no sample available.]

Occurrence	Size of exposure	Maximum radioactivity at outcrop c/s	U	Th	Remarks
A--New uranium occurrences in the migmatized biotite gneiss (bg)					
		Biotite Concentrations			
WH-3	Several m^2	4000	322	<89	
WH-4	18 by 5 cm	4750	9680	810[1/]	See Fig. 2A
WH-6	30 by 15 cm	>20,000	3070	190[1/]	See Fig. 2C
WH-10	30 by 20 cm	4000	114	120	
WH-14	45 by 30 cm	6000	99.9	<20	See Fig. 2G
WH-18	6 by 3 m	10,000	8880	<2000	See Fig. 2L
WH-20	7 by 4 m	16,000	6790	<1600	Similar to WH-18
WH-2	Several m^2	1200	---	---	Similar to WH-3
WH-5	1.5 by 0.3 m	4500	---	---	See Fig. 2B
WH-7	60 by 15 cm	3200	---	---	See Fig. 2D
WH-8	30 by 20 cm	3500	---	---	Similar to WH-7
WH-12	20 by 20 cm	4500	---	---	Similar to WH-6
WH-17	0.8 by 0.3 m	3500	---	---	See Fig. 2J
		Small Pegmatites			
WH-11	10 by 10 cm	3800	781	<170	See Fig. 2E
WH-15	1.5 by 1 m	7000	1720	<360	See Fig. 2H
WH-16	4 by 1 m	10,000	1160	<310	Similar to WH-15
		Fractures			
WH-9	1 to 2 m^2	3000	132	<24	In lens of Silver Plume Granite
WH-13	Several m^2	8000	76	<15	See Fig. 2F
B--Thorium-bearing biotite concentrations in Silver Plume Granite (sp)					
WB-20	A wedge, 12 m by 4.5 m, tapering to a point	4000	203	1480	
WB-21	A wedge, 3.5 m by 2 m tapering to a point		86.1	738	
WB-23			26.5	267	Float; see Fig. 8
WH-21		500	4.61	46.6	Silver Plume Granite
C--Thorium-bearing apatite concentration in Silver Plume Granite (sp)					
WB-12			206	8390	See mode in Table 6 and Fig. 8

Sample	Rock type	Radioactivity	Remarks
D--Miscellaneous radioactive data in the migmatized biotite gneiss (bg)			
WH-19	Mixed migmatite and pegmatite	200 c/s	Measured on outcrop
R-218		60 ppm eU	from Pearson and Johnson, 1980
R-220		50	-- Do --
R-221		500	-- Do --
R-223		50	-- Do --
R-224		160	-- Do --

[1/] Gamma ray analysis by J. S. Leventhal

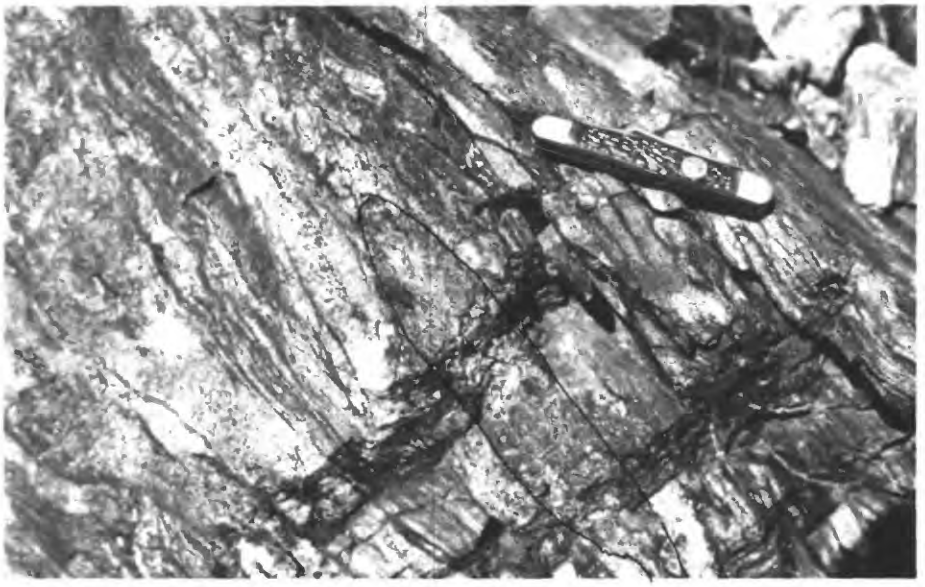

Figure 2A.--WH-4--A biotite concentration (5x18cm) in migmatite. Yellow, secondary uranium minerals and molybdenite are visible on outcrop.

Figure 2B.--WH-5--A biotite-rich migmatite (0.3x1.5m) that appears speckled because of biotite arrangement.

Figure 2C.--WH-6--A biotite concentration between pegmatite (on left) and migmatite.

Figure 2D.--WH-7--An irregular biotite concentration (15x60cm) in migmatite.

Figure 2E.--WH-11--A limonite-stained area (10x10cm) of a pegmatite.

Figure 2F.--WH-13--Fractures in a pegmatite (several m^2) filled with specular hematite.

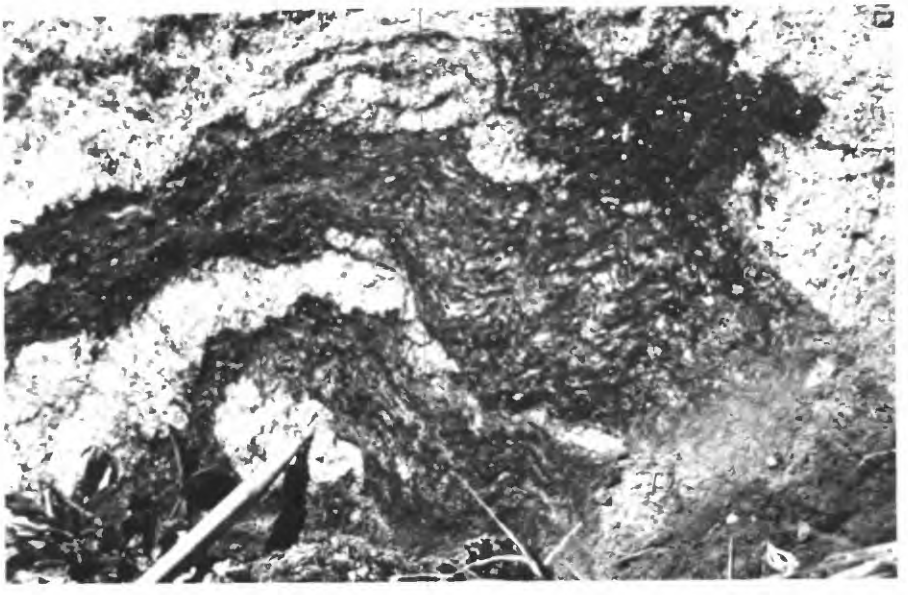

Figure 2G.--WH-14--Swirled biotite concentrations (30x45cm) in pegmatite and migmatite; abundant garnets.

Figure 2H.--WH-15--A pegmatite (1x1.5m) with radioactive areas showing yellow, secondary uranium minerals.

Figure 2J.--WH-17--A pegmatite (0.3x0.8m) with radioactive biotite concentrations. A pale blue-green skarn zone composed of an intergrowth of clinozoisite and muscovite lies between the pegmatite and hornblendite.

Figure 2K.--Close-up of blue-green skarn zone lodged between pegmatite and hornblendite; specimen is 9.5cm long.

Figure 2L.--WH-18--Radioactive biotite concentrations in a pegmatite (3x6m).

Table 2.--X-ray spectroscopic analyses of some samples from the uranium occurrences of Table 1. [Sample localities shown on Fig. 1. Analysts: J. S. Wahlberg, J. Taggart, and J. Baker. Total Fe is given as Fe_2O_3.]

	Uraniferous biotite concentrations					Uraniferous Silver Plume Granite (fractures)
	Chemical composition in weight percent					
Sample No.	WH-3	WH-6	WH-14	WH-18	WH-20	WH-9
Lab No.	D-230247	D-230248	D-230253	D-230256	D-230257	D-230249
SiO_2	50.1	34.8	46.3	47.5	42.6	68.0
Al_2O_3	20.6	19.4	28.4	18.1	28.2	17.6
Fe_2O_3	12.3	21.9	13.1	12.4	12.6	2.74
MgO	3.8	6.64	3.3	3.9	3.7	0.85
CaO	0.40	0.31	0.40	3.53	0.77	2.34
Ma_2O	2.0	<0.2	0.4	2.1	1.2	4.9
K_2O	4.03	8.26	3.72	4.30	3.75	1.65
TiO_2	1.72	3.10	1.35	1.96	1.55	0.34
P_2O_5	<0.1	0.1	<0.1	0.4	0.2	<0.1
MnO	0.09	0.12	0.17	0.11	0.13	<0.02
LOI 900°C	4.19	2.56	2.71	2.11	3.07	1.35
Total	99.33	97.39	99.95	96.41	97.77	99.89

Table 3A.--Emission spectrographic analyses from Wheeler Basin. [Semiquantitative six-step spectrographic analysis by N. M. Conklin. The following elements (detection limits given in parts per million) were looked for but not found: As, 1000; Au, 20; B, 20; Bi, 10; Cd, 50; Eu, 100; Ge, 10; Hf, 100; In, 10; Li, 100; P, 2000; Pd, 2; Pt, 50; Re, 50; Sb, 200; Ta, 500; Tb, 300; Te, 2000; Tl, 50; Tm, 20; W, 100. Sample localities shown in Fig. 1.]

A--Samples from the uranium occurrences of Table 1

		Uraniferous biotite concentrations						Uraniferous small pegmatites			Uraniferous fractures	
		WH-3	WH-6	WH-10	WH-14	WH-18	WH-20	WH-11	WH-15	WH-16	WH-9	WH-13
		Weight percent										
	Si			>10				>10	>10	>10		>10
	Al			10				7	7	7	See	7
	Fe	See Table 2 for		10		See Table 2 for		1.5	>10	1.5	Table 2	1.5
	Mg	major element		3		major element		0.05#[1]	1.5	0.5	for major	0.7
	Ca	chemistry		0.3#		chemistry		0.15#	0.2#	0.7	element	0.15#
	Na			0.7				3	0.7	1.5	chemistry	3
	K			3				3	3	1.5		3
	Ti			0.7				0.05#	0.03#	0.15		0.15
		Parts per million										
	Ag	< 0.5	<0.5	<0.5	<0.5	1.5*	1*	5*	1*	<0.5	<0.5	<0.5
	Ba	1500	1000	300	300	700	500	700	700	300	<1	<1
	Be	<1	<1	<1	<1	<1	1	<1	<1	<1	<1	<1
	Co	20	30	15	30	30	30	7	15	7	7	<7
	Cr	300	300	150	150	70	300	15	30	15	7#	30
	Cu	5#	15	30	30	5#	30	15	30	7	3#	3#
	Ga	70	70	70	30	30	70	15	15	15	30	15
	Mn	700	700	500	1500	700	1000	50#	7000	150	150	150
	Mo	150**	300**	30*	30*	1000**	300**	700**	1000**	500**	15*	20*
	Nb	70	30	30	30	30	20	<10	<10	15	15	10
	Ni	70	30	30	70	30	70	7	7	7	7	7
	Pb	200*	1500*	30	30	1500*	3000**	150	700*	500*	70	30
	Sc	30	100*	70	70	70	70	<5	200*	7	7	5
	Sn	<10	15	10	<10	15	<10	<10	<10	<10	<10	<10
	Sr	150	30#	150	30#	300	150	200	150	200	300	150
	Th†	< 89	190*††	120	<20	<2000	<1600	<170	<360	<310	<24	<15
	U†	322**	3070**	114*	99.9*	8800***	6790***	781**	1720**	1160**	132*	76*
	V	150	150	150	150	150	150	<7#	20	30	30	30
	Zn	<300	300	300	300	<300	<300	<300	<300	<300	<300	<300
	Zr	700	1500	700	300	300	700	700	150	200	300	300
Light REE	Ce	150	700*	300	<150	2000*	1000*	<150	300	200	150	<150
	La	70	300*	200	30	1500*	700*	50	300*	150	100	30
	Nd	100	300	200	<70	1500*	700*	70	200	150	100	<70
	Pr	<100	<100	<100	<100	300*	100*	<100	<100	<100	<100	<100
	Sm	<100	150*	150*	<100	300*	150*	<100	<100	<100	<100	<100
Heavy REE	Y	50	100	150	70	700*	200	300*	1000*	50	20	10
	Gd	<70	<70	<70	<70	150*	70	<70	70	<70	<70	<70
	Dy	<70	<70	<70	<70	150*	<70	70*	150*	70*	<70	<70
	Ho	<20	<20	<20	<20	20*	<20	<20	30*	<20	<20	<20
	Er	<50	<50	<50	<50	<50	<50	<50	150*	<50	<50	<50
	Lu	<50	<50	<50	<50	<50	<50	<50	50*	<50	<50	<50
	Yb	5	10	15	15	70*	20	30*	150*	30*	1.5	1

[1] Elements shown with # are depleted 0.1 or less than crustal abundance (Vinogradov, 1962). Elements shown with *, **, or *** show enrichment from 10 to 100 times, 100 to 1000 times, or greater than 1000 times crustal abundance, respectively.

† Analysis by delayed neutron activation, except as noted.

†† Gamma ray analysis.

Table 3B.--Emission spectrographic analyses from Wheeler Basin

B--Samples from Pearson and Johnson (1980)			
	Stream sediment		Altered rock
	P-012K	K-034	R-223[2]
	Weight percent		
Fe	5	5	7
Mg	0.7	0.7	0.5
Ca	1	0.7	0.07#
Ti	0.7	0.3	0.2
	Parts per million		
Ag	<0.5	<0.5	0.5
B	10	20	<10
Ba	700	500	700
Be	1	1.5	<1
Co	10	7	30
Cr	70	30	30
Cu	15	15	700*
Mn	500	700	150
Mo	15*	15*	70*
Nb	<20	<20	<20
Ni	20	20	70
Pb	100	50	10
Sc	10	7	7
Sn	30*	<10	<10
Sr	150	100	<5#
V	70	70	50
Zn	<200	<200	<200
Zr	200	150	100
La	70	150	20
Y	20	30	<10

[2] From chemical analysis As is <10 ppm, Sb <1 ppm; from atomic absorption analysis Au is <0.05 ppm, and from instrumental analysis Hg is 0.3 ppm.

Spectrographic data on these occurrences (Table 3) indicate that U and Th are not the only elements enriched by a factor of 10 or more over crustal abundance. With respect to "average crust" (Vinogradov, 1962), all of the analyzed occurrences are enriched in U and Mo, most in Pb, and some in Th, REE, Ag, and Sc. More than half the occurrences are depleted (0.1 times or less than crustal abundance) in Ca, and Na and Cu are notably low.

The following are some observations and comments about individual occurrences:

WH-4, a small biotite concentration in migmatite (Fig. 2A), displayed strong radioactivity, yellow, secondary uranium minerals, and molybdenite on the outcrop. A polished thin section of WH-4 revealed much monazite and a uraninite grain (long dimension = 1 mm) surrounded by a red-brown alteration rim, (Figure 3A). A fission track map of the uranium distribution on and around the grain is shown in Figure 3B.

WH-5 is a biotite-rich migmatite (Fig. 2B), which appears speckled because of the inhomogeneous distribution of biotite. It is 50 times the outcrop area of WH-4, but has the same level of radioactivity.

WH-6 is a biotite concentration between pegmatite and migmatite (Fig. 2C), not much bigger than WH-4, but shows intense radioactivity on the outcrop. A modal analysis of the fine-grained biotite concentration is given in Table 4. Some of the opaque micro-fracture fillings listed in the mode consist of yellow-orange, secondary uranium minerals, and some may be microgranular monazite, which was identified in a bromoform, heavy mineral separate containing mostly biotite.

Table 4.--Modal analysis of a uraniferous biotite concentration (WH-6; see Fig. 2C) in volume percent (693 point counts)

Biotite	43.7
Plagioclase (An_{25})	31.5
Muscovite (including sericite)	10.1
Opaque micro-fracture fillings	7.8
Sillimanite	6.3
Chlorite	0.4
Hematite	0.1
Zircon	trace
	99.9

Figure 3A.--Uraninite grain surrounded by a red-brown, alteration rim (long dimension = 1mm) in biotite of sample WH-4, taken in combined reflected and transmitted light.

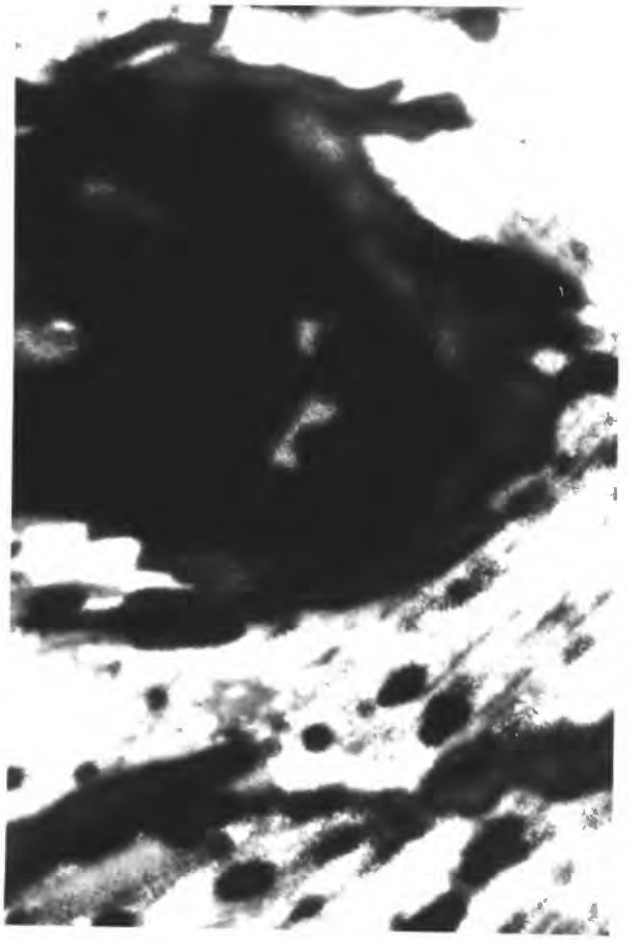

Figure 3B.--Fission track map of same uraninite grain. The fission track map consists of tracks (linear paths) developed in muscovite mica that are caused by fission fragments from U^{235} residing in the uraninite. The fissioning of U^{235} was activated by neutron flux from the USGS Triga Reactor. Irradiated 1 hr at 1000 KW.

A fission track map of WH-6 shows radioactive point sources as well as radioactive fractures in plagioclase and radioactive grain boundaries and cleavage openings in biotite and muscovite. Figures 4A, 4B, 5A, and 5B clearly show that not all fractures are uraniferous and that uranium is locally contained in fractures so small as to be not easily seen. Figures 6A and 6B show that grain boundaries and cleavage openings in biotite and muscovite are uraniferous. The intense point source in the middle of the figure is the location of a small zircon. Figures 7A and 7B show a radioactive zircon in muscovite. Biotite surrounds the muscovite. Some point sources as well as grain boundary radioactivity is evident.

WH-7 is a biotite concentration in migmatite (Fig. 2D) that is 10 times the area of WH-4, but is less radioactive.

Radioactivity in WH-9 is concentrated in fractures in a small portion of a lens of Silver Plume Granite in migmatite. The lens is about 6x9 meters in size and chemically is closer to quartz monzonite than to granite (Table 2; see also Young and Olhoeft, 1976). A fission track map of the radioactive part of the Silver Plume Granite shows some point sources of radioactivity (monazite and zircon), but most radioactivity emanates from microfractures in feldspar, quartz, and chloritized biotite.

WH-11 is a small, radioactive, limonite-stained area of a pegmatite (Fig. 2E). Besides being enriched in U, Mo, Th, and Ag it is also enriched in the heavy REE (Table 3).

WH-13 is a pegmatite with many fractures (Fig. 2F), some of which are filled with specular hematite. Little or no biotite is present. A bromoform, heavy mineral separation yielded black specularite, red hematite, and chlorite, part of which shows a triangular network of inclusions (hematite?).

WH-14 consists of swirled biotite concentrations, which contain abundant garnet and sillimanite, in pegmatite and migmatite (Fig. 2G).

WH-15 is a pegmatite (Fig. 2H), in migmatite, that contains several radioactive areas, on which yellow secondary uranium minerals may be seen. It is similar to WH-11 in that it is enriched in U, Mo, Pb, Ag, Sc, and the heavy REE (Table 3).

WH-16 is a pegmatite in migmatite. Most of the radioactivity in the pegmatite comes from small biotite concentrations, stained by yellow secondary uranium minerals.

WH-17 is a pegmatite with radioactive biotite concentrations. The pegmatite is in hornblendite and a pale blue-green band (Figs. 2J and 2K), several centimeters thick, lies between the pegmatite and the hornblendite. Thin sections of the blue-green band, which is a skarn or reaction zone between the two rock types, shows it to be a very fine grained intergrowth of rosettes of clinozoisite and muscovite. A modal analysis of the blue-green band is given in Table 5.

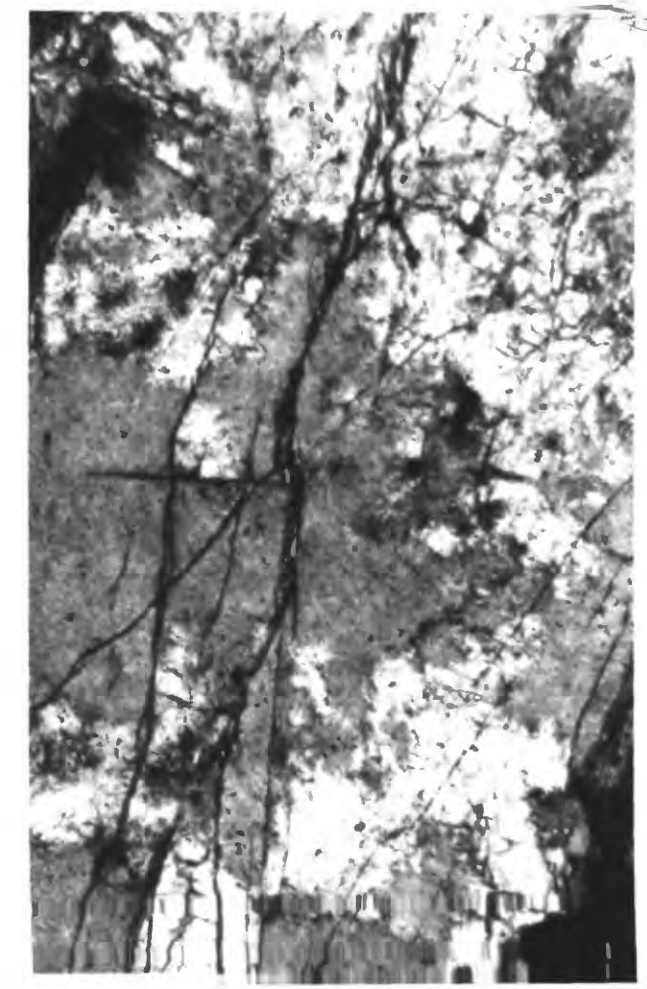

Figure 4A.--Fractures in plagioclase (long dimension of photomicrograph = 5.5mm) in sample WH-6.

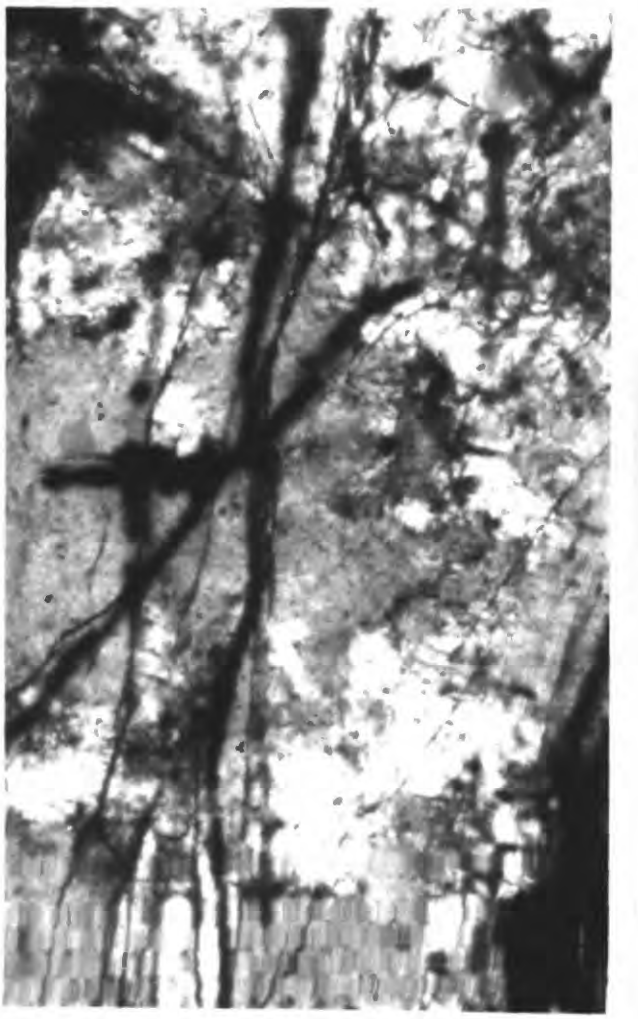

Figure 4B.--Fission track map of same scene. Note radiation-free fractures and radiation emanating from insignificant fractures. Irradiated 4 hr at 1000 KW.

Figure 5A.--Magnification of portion of Figure 4A (long dimension of photomicrograph = 1.7mm).

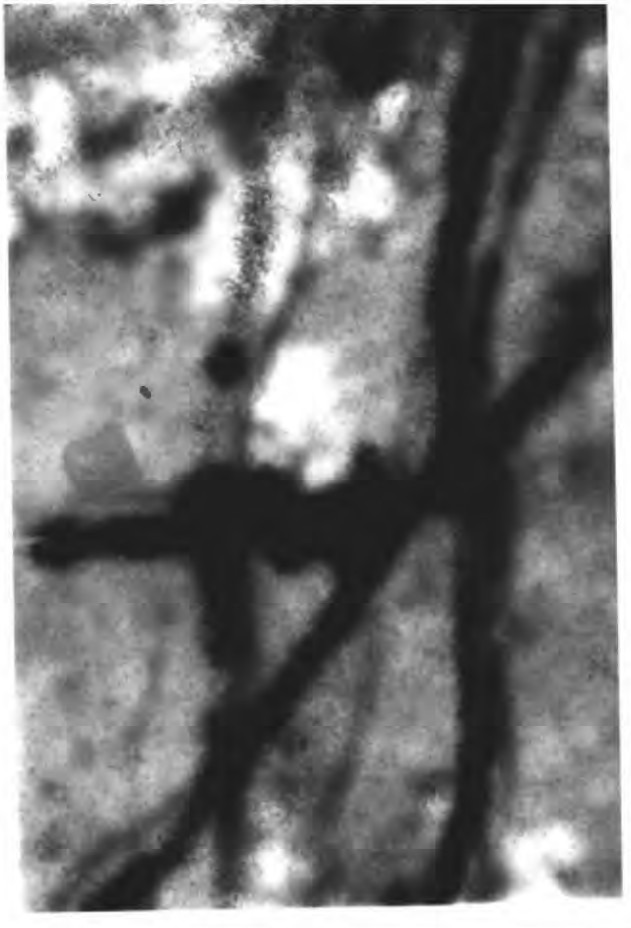

Figure 5B.--Fission track map of same scene.

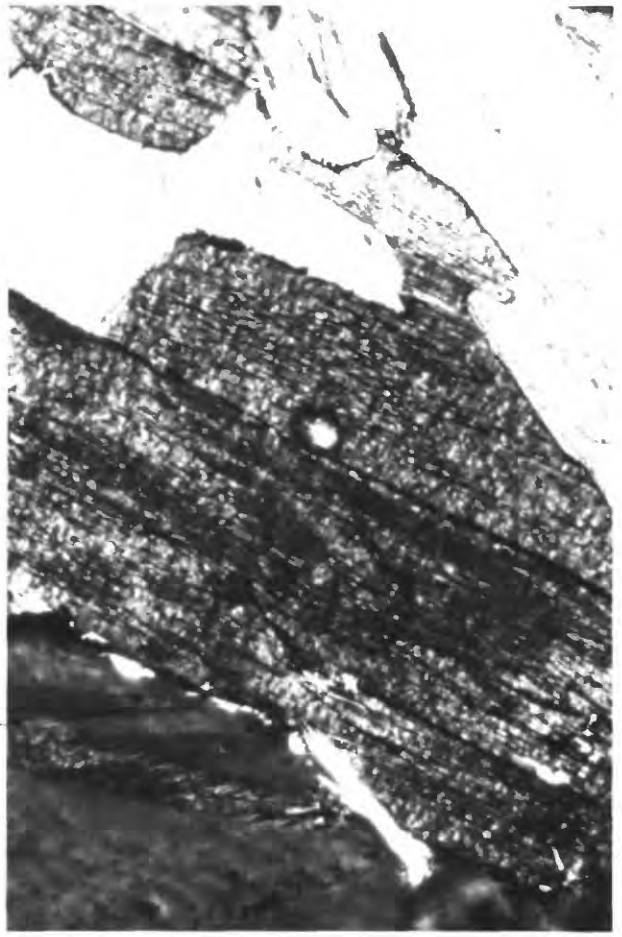

Figure 6A.--Biotite and muscovite (small zircon in biotite) in sample WH-6. Long dimension of photomicrograph = 1.7mm.

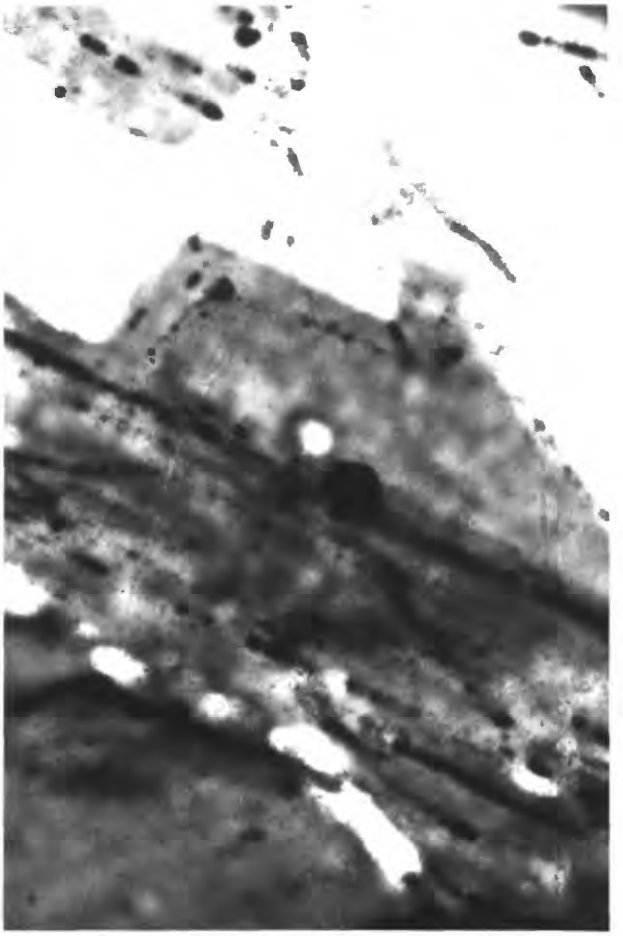

Figure 6B.--Fission track map of same scene, but shifted slightly to show that grain boundaries and cleavage openings are uraniferous. Note intense activity from zircon. Irradiated 4 hr at 1000 KW.

Figure 7A.--Zircon in muscovite that is surrounded with biotite (long dimension of photomicrograph = 0.87mm) in sample WH-6.

Figure 7B.--Fission track map of same scene. Note radioactivity from grain boundaries, as well as point sources. Irradiated 4 hr at 1000 KW.

Table 5.--Modal analysis of blue-green band of WH-17 in volume percent (503 point counts)

Clinozoisite	61.8
Muscovite	24.5
Epidote	6.8
Quartz	3.6
Chlorite	1.8
Calcite	1.0
Apatite	0.4
Dusty opaque	0.2
Allanite	Trace
	100.1

WH-18 (Fig. 2L) and WH-20 are the most uraniferous of the occurrences. Both are characterized by radioactive concentrations within pegmatite. Yellow secondary uranium minerals are readily seen and both occurrences are enriched in U, Mo, Pb, Th, Ag, and REE, with the light REE dominant (Table 3).

Thorium anomalies in the Silver Plume Granite

The radioactive anomalies found in the Silver Plume Granite (Fig. 1) are indistinguishable in appearance from the radioactive biotite concentrations found in the migmatized biotite gneiss of Wheeler Basin. The difference, however, is that the anomalies in the Silver Plume Granite are due to monazite rather than uraninite, and therefore Th values are much higher than U values (Table 1).

The largest of the biotite concentrations is represented by sample WB-20. In a very steep couloir the biotite concentration appeared as a wedge about 12 m long terminating downward in a point. At its highest exposure the thickness of the wedge was about 4.5 m, where it displayed a lens at right angles to the wedge for at least another 5 m. Highest counts on the outcrop were 4000 c/s. A smaller, but similar wedge-shaped outcrop of biotite concentration, about 3.5 by 2 m, is represented by sample WB-21. Only a few other smaller bodies of biotite concentrations were seen in place, but float boulders and cobbles of biotite concentrations were found in the general area, presumably originating in higher, inaccessible parts of the steep couloirs.

The biotite in concentrations is mostly medium grained, but locally is coarse grained and has no preferred orientation. Sharp contacts generally are seen with the host, Silver Plume Granite. Magnetite, monazite and apatite are important accessory minerals as shown by modal analysis (Table 6). Delayed neutron analyses (Table 1) indicate that Th is 7 to 10 times greater than U,

Table 6.--Modal analyses of Silver Plume Granite, biotite concentrations in the Silver Plume Granite, and an apatite concentration in the Silver Plume Granite in volume percent

	Silver Plume Granite				Biotite concentrations			Apatite concentration
	WB-4[1]	WB-9	WB-10	WH-21	WB-20[2]	WB-21	WB-23[3]	WB-12[4]
Quartz	38.7	27.1	37.4	25.6	0.1	0.1	3.9	---
Plagioclase, (sericitized)	15.9 (An_{15})	42.0 (An_{15})	20.3 (An_{15})	23.6 An_{15})	---	29.5 (An_{28})	---	---
Microcline	36.8	21.3	34.9	40.8	---	---	---	---
Biotite	6.1	5.2	4.6	1.9	71.7	52.1	62.2	---
Muscovite	0.8	2.7	0.5	1.9	6.7	0.9	8.8	tr
Chlorite	0.9	0.6	2.0	4.0	---	0.1	---	---
Magnetite	---	---	---	---	16.1	7.9	15.6	9
Blackopaque	0.5	1.0	0.2	2.1	---	---	---	---
Red hematite	---	---	---	---	1.3	1.1	0.4	---
Monazite	0.3	tr	0.3	---	3.7	0.9	2.0	8
Apatite	tr	---	tr	tr	---	6.3	6.4	82
Zircon	tr	tr	tr	tr	0.1	0.4	0.7	1
Sphene	---	---	---	---	---	0.1	tr	---
Sillimanite	tr	tr	tr	---	0.1	0.5	---	---
Total	100.0	99.9	100.2	99.9	99.8	99.9	100.0	100
Point Counts	636	667	660	618	676	844	1368	790

[1] Radioactivity at outcrop is 620-830 c/s. [2] Radioactivity at outcrop is 4000 c/s. [3] Float.
[4] Exact locality is not known, but WB-12 is presumed to come from the same couloir as that of WB-21, where it was collected by Delmer L. Brown, who observed lenslike segregations of medium-grained apatite concentrations dipping 25°-30° eastward and about 4.5 by 0.6 m in size, surrounded by Silver Plume Granite.

and Table 7 indicates that Mo and Pb are much lower than Mo and Pb values in biotite concentrations in migmatized biotite gneiss. Table 8 gives the chemical composition of one of the biotite concentrations.

The Silver Plume Granite is fine to medium grained and varies from buff to pale pink to gray-white. Modal analyses (Table 6) indicate that the composition varies from quartz monzonite to granite. A fission track map of WH-21 shows only point sources of radioactivity from accessory minerals. Several other data points, shown on figure 1, complete radioactive information within the Silver Plume Granite: These are: R-219, collected by Pearson and Johnson (1980), yielded an eU of 30 ppm, and WB-5 and WB-6 are from outcrops where I recorded 500-680 c/s and 700-900 c/s, respectively. Outcrops of migmatite and banded gneiss next to WB-6 yielded 300-320 c/s.

The apatite concentration, WB-12, apparently is an extreme form of concentration of apatite, magnetite, and monazite. Unfortunately, its exact locality is not known--see Note 4 in Table 6. Figure 8 shows specimens of WB-12 and WB-23, the biotite concentration that is closest to WB-12 in composition. The apatite of WB-12 is equigranular and medium grained. Monazite and magnetite tend to occur at grain boundaries of the apatite and are smaller in size. The apatite is colorless, but contains many dusty opaque inclusions, especially concentrated in linear zones that may be healed fractures. The apatite is apparently fluorapatite as $\omega = 1.636 \pm 0.001$ and $\varepsilon = 1.633 \pm 0.001$. From spectrographic analysis of WB-12 (Table 7) the REE content appears to be too high to be accounted for by the monazite (8% modal--see Table 6), hence it is reasonable to assume that the apatite contains some REE. Unit cell parameters of the fluorapatite, obtained by Phoebe Hauff, are as follows:

$$a = 9.368\text{Å} \pm 0.0013\text{Å}$$
$$c = 6.871\text{Å} \pm 0.0016\text{Å}$$
$$\text{volume} = 523.43\text{Å}^3.$$

Mysen and others (1981) made a laboratory study of phosphorus in silicate melts, but as far as I know, few, if any, concentrations of such extremely phosphatic composition, as represented by WB-12, have been found in granite.

CONCLUSION

Present observations indicate that uranium is more abundant in biotite concentrations in migmatized biotite gneiss than in biotite concentrations in Silver Plume Granite, which suggests that uranium was originally in the pre-1,700-m.y. metamorphic complex and was remobilized by heat and pressure at the time of the Silver Plume Granite intrusion (1.4 b.y.) and segregated in biotite concentrations. It seems likely that the Silver Plume Granite did not supply the uranium as biotite concentrations in the Silver Plume Granite are thorium-rich rather than uranium-rich.

Remobilization of uranium in metamorphic rocks, as found in Wheeler Basin, seems to be exemplified on a much larger and economic scale in the Rössing uranium deposit of South West Africa (Smith, 1965, and Berning and others, 1976).

Table 7.--Emission spectrographic analyses of biotite concentrations in the Silver Plume Granite and of an apatite concentration in the Silver Plume Granite. [Semiquantitative six-step spectrographic analysis by N. M. Conklin. The following elements (detection limits given in parts per million) were looked for but not found: As, 1000; Au, 20; B, 20; Be, 1.5; Bi, 10; Cd, 50; Ge, 10; Hf, 100; In, 10; Pd, 2; Pt, 50; Re, 50; Sb, 200; Ta, 500; Te, 2000; Tl, 50; U, 500; W, 100. Sample localities shown in Fig. 1, except for WB-12, the apatite concentration.]

	Biotite concentrations			Apatite concentration
	WB-20	WB-23	77-82	WB-12
	Weight percent			
Si	10		10	0.2#
Al	7		7	0.7#
Fe	>10	See	>10	7
Mg	3	Table 8	3	0.07#
Ca	0.07#[1]	for major	0.07	>10
Na	0.15#	element	0.15#	0.15#
K	7	chemistry	7	--[2]
Ti	1.5		1.5	0.3
P	<0.2		<0.2	>10**
	Parts per million			
Ag	1*	<0.5	<0.5	30**
Ba	500	300	300	7#
Co	20	30	30	<5
Cr	150	150	150	<50
Cu	150	50	200	20
Ga	70	100	100	70
Mn	700	700	1500	3000
Mo	<10	<10	7	<10
Nb	70	100	100	<10
Ni	30	70	50	<5#
Pb	70	<10	150	700*
Sc	150*	70	30	<70
Sn	30*	30*	30	<10
Sr	15#	7#	15#	150
Th	1480†**	267†*	1500**	8390†**
U	203†*	26.5†*	--	206†*
V	150	300	150	150
Zn	<200	300	<500	<200
Zr	1500	300	2000*	1500
Ce	3000*	300	3000*	30000**
Eu	<100	<100	<100	100*
La	3000**	150	3000**	20000**
Nd	3000*	150	3000*	15000**
Pr	700*	<100	700*	7000**
Sm	700*	<100	700*	3000***
Y	200	30	500*	5000**
Gd	150*	<70	150*	3000**
Dy	<70	<70	150*	1500**
Ho	<20	<20	<20	200*
Er	<50	<50	<50	<200
Lu	<50	<50	<50	<200
Yb	15	3	15	300*
Tm	<50	<50	<50	<100

[1] Elements shown with # are depleted 0.1 or less than crustal abundance (Vinogradov, 1962). Elements shown with *, **, or *** show enrichment from 10 to 100 times, 100 to 1000 times, or greater than 1000 times crustal abundance, respectively.

[2] Not looked for.

† Analysis by delayed neutron activation.

Table 8.--X-ray spectroscopic analysis of a biotite concentration in Silver Plume Granite. [Sample locality shown on Fig. 1. Analysts: J. S. Wahlberg, J. Taggart, and J. Baker. Total Fe is given as Fe_2O_3.]

Chemical composition in weight percent	
Sample No.	WB-23
Lab No.	D-230259
SiO_2	36.7
Al_2O_3	19.8
Fe_2O_3	21.0
MgO	6.95
CaO	0.13
Na_2O	<0.2
K_2O	9.56
TiO_2	2.51
P_2O_5	0.1
MnO	0.13
LoI 900°C	1.51
Total	98.59

Figure 8.--A specimen from WB-23 (on right) biotite concentration, containing 16 percent magnetite and 6 percent apatite (long dimension of WB-23 = 5.5cm), compared with two pieces of WB-12, apatite concentration.

REFERENCES CITED

Berning, J., Cooke, R., Hiemstra, S. A., and Hoffman, U., 1976, The Rössing Uranium deposit, South West Africa: Economic Geology, v. 71, no. 1, p. 351-368.

Ludwig, K. R., and Young, E. J., 1975, Absolute age of disseminated uraninite in Wheeler Basin, Grand County, Colorado: U.S. Geological Survey Journal of Research, v. 3, no. 6 p. 747-751.

Mysen, B. O., Ryerson, F. J., and Virgo, D., 1981, The structural role of phosphorus in silicate melts: American Mineralogist, v. 66, p. 106-117.

Pearson, R. C., and Johnson, G., 1980, Mineral resources of the Indian Peaks Study Area, Boulder and Grand Counties, Colorado: U.S. Geological Survey Bulletin, 1463, 109 p.

Smith, D. A. M., 1965, The geology of the area around the Kahn and Swakop Rivers in South West Africa: South Africa Geological Survey Memoir, South West Africa Ser. 3, 113 p.

Tweto, Ogden, 1977, Nomenclature of Precambrian rocks in Colorado: U.S. Geological Survey Bulletin, 1422 D, 22 p.

Vinogradov, A. P., 1962, Average contents of chemical elements in the principal types of igneous rocks of the earth's crust: Geochemistry, no. 7, p. 641-664.

Young, E. J., and Hauff, P. L., 1975, An occurrence of disseminated unaninite in Wheeler Basin, Grand County, Colorado: U.S. Geological Survey Journal of Research, v. 3, no. 3, p. 305-311.

Young, E. J., and Olhoeft, G. R., 1976, Relations between specific gravity and chemical composition for a suite of igneous and metamorphic rocks: U.S. Geological Survey Open-File Report 76-809, 12 p.